Rheol Acta (2001) 40: 104–110

ORIGINAL CONTRIBUTION

Sabrina Pricl
Maurizio Fermeglia

Virtual rheological experiments on linear alkane chains confined between titanium walls

Received: 1 January 2000
Accepted: 7 November 2000

Paper presented at the Southern Europe Conference on Rheology – Eurorheo 99-3, 7–11 September 1999, Falerna, Italy.

S. Pricl (✉) · M. Fermeglia
Computer-Aided Systems Laboratory
Department of Chemical Environmental and Raw Materials Engineering
University of Trieste
Piazzale Europa 1
I-34127 Trieste, Italy
e-mail: sabrinap@dicamp.univ.trieste.it

Abstract Molecular dynamics simulations are used to investigate the rheological behavior of confined linear alkane chains under shear flow conditions. The simulated fluids are contained between atomistic, pure titanium walls, coupled to an external bath to maintain the temperature at a constant value. Shear flow conditions are imparted by moving the metal walls in opposite directions, and the corresponding density, velocity, and temperature profiles of the systems are calculated. For the shear rates investigated, all linear alkane chains exhibit a tendency for slip at the walls, evidenced by density profiles divided into two distinct regions and small discontinuities in the velocity and temperature profiles at the wall/fluid interface. Compared to equilibrium, alkane chains show higher mean-square end-to-end distances, characterized by higher components along the shear flow direction.

Key words Molecular simulations · Confined chain rheology · Molecular dynamics · Metal surfaces

Introduction

The behavior of confined molecular liquids in shear flow is of importance in industrial applications, ranging from the formulation of effective lubricating systems to polymer extrusion and processing operations. In engineering applications, the flow properties of any given system are usually modeled using macroscopic equations, the solution of which requires the specification of appropriate boundary conditions and the corresponding numerical values of some transport coefficients, such as viscosity and thermal conductivity. The most commonly employed boundary condition, however, is that the wall and the fluid layer next to it move at the same velocity; in other words, no-slip (or stick) phenomena take place at the shearing walls. Further, continuum mechanics analyses often assume that the transport coefficients of the confined fluids are the same as those of a bulk fluid. Recent experiments have called these assumptions into question (Kalika and Denn 1987). Indeed, on the microscopic scale, a liquid film confined between two solid surfaces decreases its thickness and eventually stabilizes at a finite thickness of a few molecular diameters. An extraordinary large pressure is then needed to squeeze out the final few layers of liquid between the two solid surfaces. This experiment's simplicity belies its far-reaching implications: when the thickness of a liquid film becomes comparable to molecular dimensions, classical intuition based on continuum properties inexorably fails.

Previously published computer simulation studies on confined fluids of chain molecules have highlighted the tendency of a fluid to form layers of variable density in the direction normal to the surface (Luedtke and Landman 1992; Gao et al. 1997; Khare et al. 1996; Granick 1999). Most of these works, however, can be broadly classified into two major categories: the homogeneous shear and the surface driven shear methods. In the former case (Evans and Morriss 1990), the shear flow conditions are simulated by modifying the equations of motions of the molecules and using sliding wall periodic boundary conditions; accordingly, this technique is more

suitable for simulating small regions of a bulk fluid under shear. The surface driven simulation method is based on the concept that the shear is imparted on the material via the actual motion of the confining walls, therefore making this approach more attractive for this type of study (Bitsanis et al. 1987, 1990). In our opinion, however, the simulation studies of confined fluids under shear appeared to suffer from at least two major limitations. To begin with, in both methods a constant temperature is imposed throughout the fluid. As we shall see later in the discussion section, such conditions are obviously unrealistic under the extremely high values of the shear rate realized in these experiments. Second, in almost all works the so-called united atom approximation is used to model the molecular fluids, in which a suitable group of atoms (e.g., a methylene group in the case of an alkane chain), is lumped into single ''quasi-atoms'' of appropriate size.

Therefore, the long term goal of our work is to employ fully atomistic molecular mechanics/molecular dynamics simulations (MM/MD) to set a bridge between the micro- and the macroscopic pictures of flow behavior, thereby providing some insight into atomistic scale hydrodynamics near the surface as well as the effects of confinement on transport properties.

Computational approach

All simulations were run on a Silicon Graphics Origin 200 (microprocessor MIPS RISC 10000, 64 bit CPU, 128 MB RAM) and performed by using the commercial software Cerius^2 (v. 3.9) from Molecular Simulation Inc. (for both MM and MD simulations) and in-house developed computer programs (stand-alone and add-on to the commercial package). The generation of accurate model structures of the alkane chains considered (*n*-decane, *n*-pentadecane, and *n*-eicosane) was conducted as follows. First each molecule was built and its geometry optimized via energy minimization using the COMPASS force field. The COMPASS FF is the first ab initio force field that has been parametrized and validated using condensed-phase properties in addition to various ab initio and empirical data for molecules in isolation (Sun and Rigby 1997). The bond terms of the COMPASS FF potential energy function include a quartic polynomial both for bond stretching and angle bending, a three-term Fourier expansion for torsions, and a Wilson out-of-plane coordinate term. Six cross-terms up through the third order are present to account for coupling between the intramolecular coordinates. The final two nonbonded terms represent the intermolecular electrostatic energy and the van der Waals interactions, respectively; the latter employs an inverse ninth power term for the repulsive part rather than the more customary 12th power term (see Appendix for details).

The molecules were modeled to have a total charge equal to zero, and the distribution of the partial charge within each molecule was determined by the charge equilibration method of Rappé and Goddard (1991). Energy was minimized by up to 5000 Newton-Raphson iterations. Following this procedure, the root-mean-square (rms) atomic derivatives in the low energy regions were smaller than 0.05 kcal/mole Å. Long-range nonbonded interactions were treated by applying a cut-off length of 20 Å, and to avoid the discontinuities caused by direct cutoffs, the cubic spline switching method was used (Brooks et al. 1985). van der Waals distances and energy parameters for nonbonded interactions between heteronuclear atoms were obtained by the sixth-power combination rule proposed by Waldman and Hagler (1993).

The amorphous structures for each ensemble of alkane chains were generated and packed into a cubic simulation box with 3-D periodicity. The structures were then relaxed to minimize energy and avoid atom overlaps using the conjugate-gradient method. In each case, the Ewald technique was employed in handling nonbonded interactions and the charge equilibration method was again used to equilibrate the charge distribution.

The shearing walls consisted of a series of layers of pure titanium atoms attached at face-centered cubic (FCC) lattice sites (see Fig. 1). In our coordinate systems, the walls were parallel to the xy plane and were separated by a distance H in the z direction, and periodic boundary conditions were used both in the x and y directions.

Simple shear conditions were imposed on the system by moving the metal walls at constant velocity. The two walls were moved with the same velocity but in opposite directions along the x-axis. The value of the shear rate $\dot{\gamma}$ could be calculated by considering how our model was mapped onto a real fluid; accordingly, the nominal value was 7.9×10^9 s^{-1}.

The wall temperature was kept constant at $T_{wall} = 460$ K by coupling the motion of the metal wall atoms to a heath bath (Berendsen et al. 1984). Pressure was kept constant by coupling to a pressure bath (Andersen 1980), with relaxation time $\tau_P = 0.1$ ps. The pressure tensor **P** is expressed in terms of molecular quantities by

$$\underline{\mathbf{P}}V = \sum_{i=1}^{N} \frac{\mathbf{p}_i \mathbf{p}_j}{M} + \sum_{1 \le i} \sum_{\le j < N} \mathbf{r}_{ij} \mathbf{F}_{ij}$$

where V is the volume of the system, $\mathbf{r}_{ij} = \mathbf{r}_i - \mathbf{r}_j$ is the vector joining the centers of the molecules i and j, and $\mathbf{F}_{ij}$ is the force between them.

The Newton molecular equations of motion were solved by the Verlet leapfrog algorithm (Verlet 1967), using an integration step of 1 fs. Since the partial charges assigned by the charge equilibration

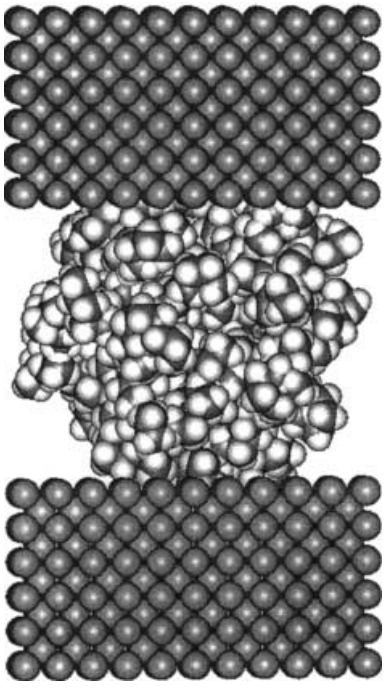

Fig. 1 Molecular drawing of the simulated systems

method are dependent on structure geometry, they were updated regularly every 100 MD steps during the entire MD runs.

All simulations consist of an equilibration stage of 300 ps, followed by a production run of at least 700 ps. All properties of the system are confirmed to be time independent and symmetric about the central plane of the fluid film. The molecular model places constraints on the size of the simulation cell because there have to be an integral number of rows of wall atoms in the x and y directions and an integral number of chains. The simulations for 100 alkane chains performed in this work employed a box with suitable dimensions so that the separation between the walls was fixed at $H = 51$ Å. An example of the simulation cell employed is given in Fig. 2 for the *n*-decane molecules.

Results and discussion

Density, velocity, and temperature profiles of the linear alkanes

The validity of any molecular simulation rests on the suitability and accuracy of the equations used for the intermolecular potentials. Although the accuracy of a prediction may be estimated by considering the approximations and simplifications of the model and computational procedure, the final test lies in a comparison of theoretically predicted and experimentally measured properties. Table 1 reports, as an example, the results of this comparison in terms of geometrical molecular parameters.

From an inspection of the values reported in Table 1 we can conclude that the agreement is more than satisfactory.

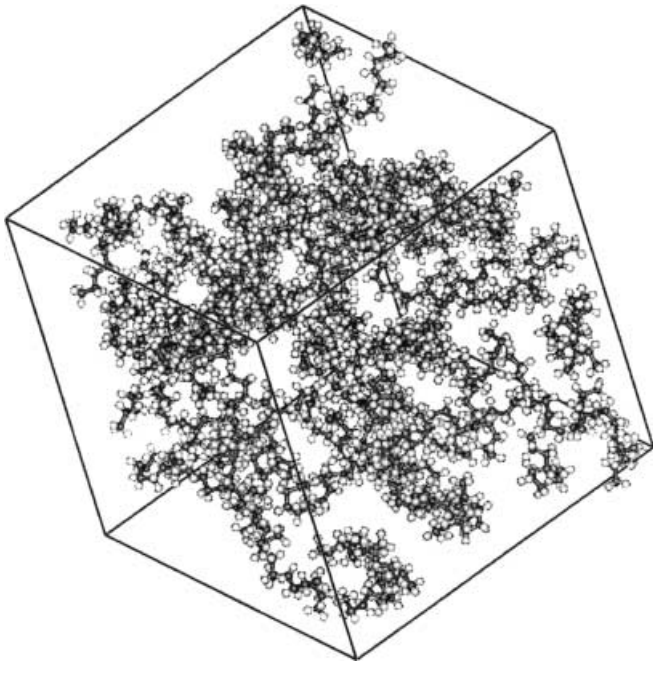

Fig. 2 Simulation cell employed for 100 molecules of *n*-decane

Table 1 Structural molecular parameters for *n*-decane. Comparison between calculated and experimental values (in parenthesis, where available)

Bond	Bond length (Å)	Angle	Bond Angle (°)
C-C in CH_2-CH_2	1.526 (1.530)	C-C-C	112.2 (112)
C-C in CH_3-CH_2	1.519 (1.520)	H-C-H	106.8 (107)
C-H	1.107 (1.107)		

We performed a further check of the agreement between simulation and experiment by comparing the simulated PVT behavior of the three alkanes considered. As can be seen from Fig. 3, the agreement between real and virtual molecules is again excellent, thus confirming the validity of the force field choice.

Accordingly, we begin our analysis of the rheological experiments by considering the site density profiles of the alkane chains under shear. Figure 4 depicts, as an example, the density profile obtained for *n*-eicosane at the shear rate $\dot{\gamma} = 7.9 \times 10^9$ s^{-1} and $T_{wall} = 460$ K. In this figure, wall atoms are attached to lattice sites at $z = 0$ and 51, and the density profiles are normalized by the average density between $z = 0$ and 51. Since in simulated systems the definition of the average fluid density ρ can be rather ambiguous, we calculated ρ by assuming that the fluid cannot occupy a volume equal to half the Lennard-Jones length parameter σ at either wall since the wall atoms effectively exclude the fluid from this region.

In Fig. 4, the fluid is seen to be divided into two distinct regions: a wall-fluid interfacial region, where the walls induce significant ordering, and a bulk-like, homogeneous fluid region in the central part of the film. Furthermore, at least three well-defined fluid layers next to the walls are observed for these simple alkane, which may reasonably ascribed to a molecular efficient packing (see Fig. 4). All three linear alkanes exhibit the same density profile; small differences were detected only in the height of the first density peak, which slightly decreases as the molecular weight of the linear alkane increases. Similar results have been reported in literature for other simple fluids (Khare et al. 1996).

Now, for no-slip boundary condition and Couette flow, continuum mechanics predicts a linear velocity profile between the surfaces. Figure 5 compares the velocity profiles obtained by simulation to those predicted by continuum mechanics for *n*-decane. As may be concluded from this Figure, there is no discontinuity in the velocity profile which, except for a region of small thickness near the wall, is linear over the entire channel. Since all molecules considered show the same velocity profiles, we can conclude that this set of short alkane chains show little tendency for slip at the wall, consistent with the previous evidence on density.

The final evidence for slip-at-the-wall condition comes from an inspection of the temperature profiles

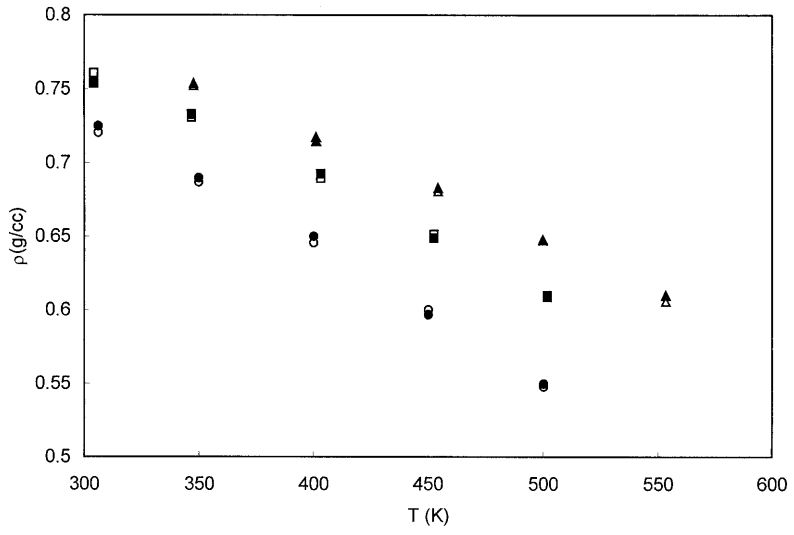

Fig. 3 Comparison between experimental (*open symbols*) and MD predicted PVT behavior (*filled symbols*) of the three alkanes considered. ○ and ●: *n*-decane; □ and ■: *n*-pentadecane; △ and ▲: *n*-eicosane

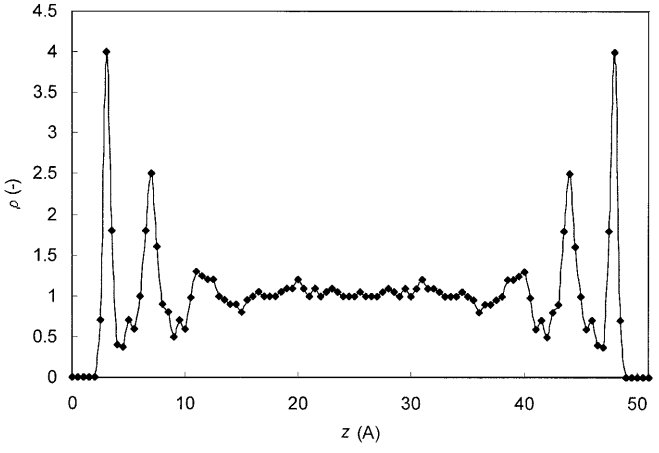

Fig. 4 Normalized density profile obtained for *n*-eicosane ($T_{wall} = 460$ K, $P = 20$ MPa, $H = 51$ Å, $\dot{\gamma} = 7.9 \times 10^9$ s^{-1}). The continuous lines serve as a guide for the eye

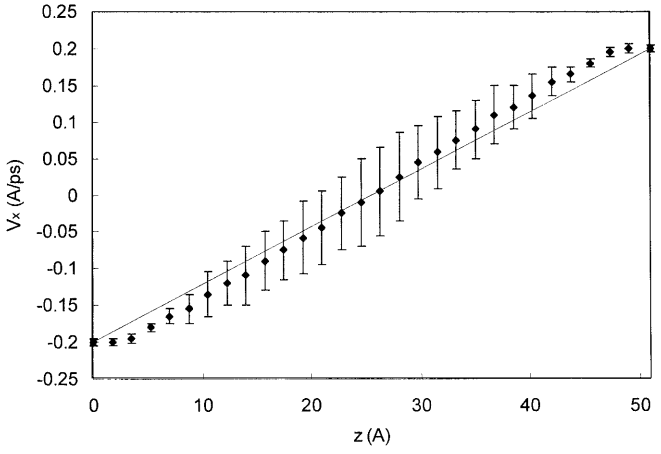

Fig. 5 Velocity profile obtained for *n*-decane ($T_{wall} = 460$ K, $P = 20$ MPa, $H = 51$ Å, $\dot{\gamma} = 7.9 \times 10^9$ s^{-1})

exhibited by these simple fluids. Figure 6 shows that the temperature profile for *n*-pentadecane under shear is roughly parabolic, as again expected from continuum mechanics. Nonetheless, a small temperature drop is observed at the walls, which is again consistent with the contained velocity slip reported above. At this stage we must point out that, in canonical virtual experiments on confined fluids, the constant temperature is imposed across the entire fluid (Evans and Morriss 1990). At very high shear rates, such as those corresponding to the conditions employed in our case, this thermal coupling is not realistic, because the viscous heat generated in the fluid is artificially and immediately removed, and this would only take place in a fluid characterized by an infinite thermal conductivity. The simulation conditions we adopted mimic more closely a true experimental setup since the unique temperature control we provide is

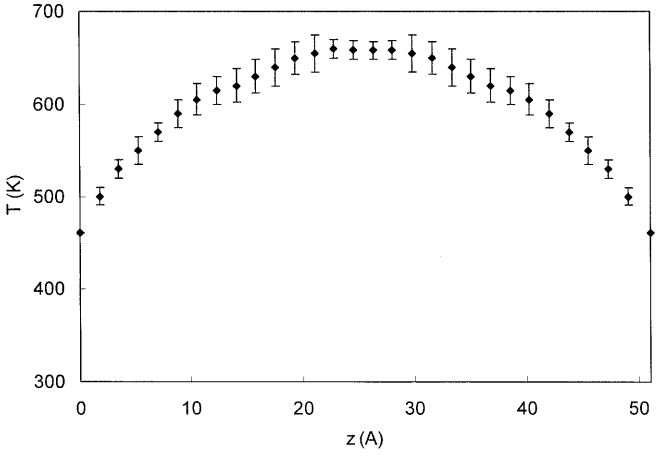

Fig. 6 Temperature profile obtained for *n*-pentadecane ($T_{wall} = 460$ K, $P = 20$ MPa, $H = 51$ Å, $\dot{\gamma} = 7.9 \times 10^9$ s^{-1})

by coupling between the walls and the heat bath. Accordingly, we may observe that the temperature rise is rather high for this fluid thickness. This result is reasonable and can be physically explained by considering that the only outlet for the viscous heat generation in the system is through the walls, which are held at a constant temperature as explained above. Since the walls are quite far apart, heat removal by conduction to the walls is not so efficient.

Conformational properties under flow

The presence of imposed shear conditions and of metal surfaces are clearly expected to influence the molecular dimensions of the considered compounds if compared to those of the corresponding bulk fluids. As a piece of evidence, we report in Fig. 7 the comparison between the root-mean-square end-to-end distance $\langle r^2 \rangle^{1/2}$ obtained from simulation for *n*-decane chains under shear and at equilibrium, respectively. The end-to-end distance is the straight-line distance between the ends of a linear molecule in a given conformation. It can obviously change with the overall molecular shape and will vary with time if the molecule is dynamically flexible. We can see from this figure how sheared molecules present higher dimensions with respect to unsheared ones at any given distance from the walls.

If we now consider that the three flow directions are not equivalent, it could be enlightening to analyze the components of the mean-square end-to-end distance separately. Indeed, Fig. 8 shows that, in the flow direction (x), the dimensions of the sheared alkanes are decidedly higher than those of the corresponding unsheared system.

On the other hand, a comparison of the other two components of $\langle r^2 \rangle^{1/2}$ (the vorticity direction y and the shear gradient direction z, respectively) shows that the effects exerted by flow in these directions are not as marked as they are for the remaining component. This expected results is illustrated, again for *n*-decane, in Fig. 9.

A closer inspection of these last three figures yields further matters for discussion. Beyond a region of given thickness from the walls, all three components of $\langle r^2 \rangle^{1/2}$ are characterized by the same magnitude under equilibrium conditions. However, it is not so when a shear is applied since, again as expected, the y component shows higher values and the z component shows lower values (compared to bulk), both under equilibrium and shear. This evidence could be reasonably ascribed to a flattening and/or a reorientation process of the chains near the walls. Indeed, a previous detailed and accurate study (Khare et al. 1996) has revealed that, in the near proximity of the wall surface, the molecular bonds are

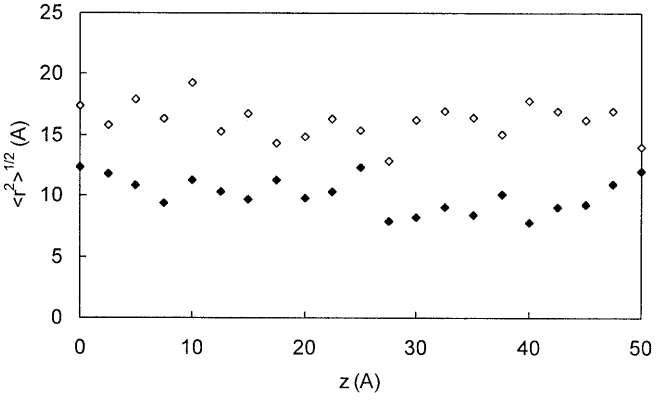

Fig. 7 Comparison of the mean-square end-to-end distance obtained under shear (*open symbols*) and under equilibrium (*filled symbols*) for *n*-decane

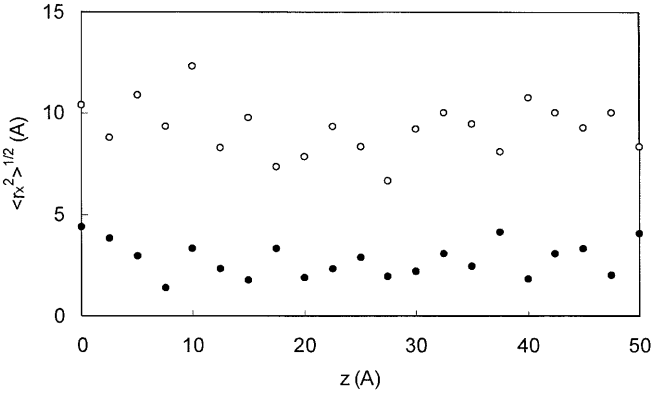

Fig. 8 Comparison of the x-component of the mean-square end-to-end distance obtained under shear (*open symbols*) and under equilibrium (*filled symbols*) for *n*-decane

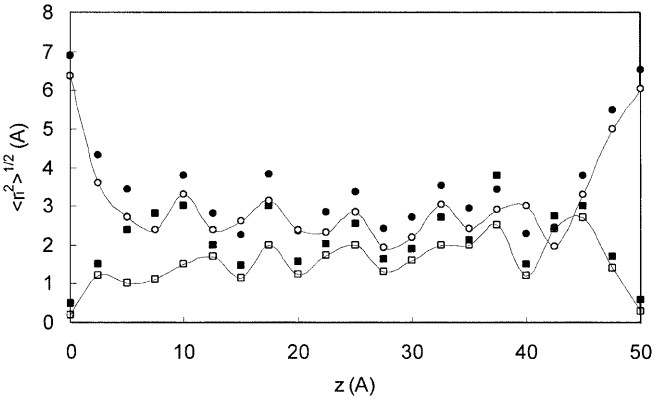

Fig. 9 Comparison of the y- and z-components of the mean-square end-to-end distance obtained under shear and under equilibrium for *n*-decane. y-component: under shear (○), under equilibrium (●); z-component: under shear (open squares), under equilibrium (■). The continuous lines serve as a guide for the eye

oriented parallel to the wall both at equilibrium and under shear. Away from the walls, bonds have an isotropic orientation at equilibrium while, under shear, the orientational correlation function values indicate that, on average, individual bonds have a slight tendency to align parallel to the wall at all distances.

Conclusions

In this paper we report the results of a molecular dynamics simulation study of the shear flow behavior of linear alkane chains confined in films between pure titanium surfaces. All the molecules considered show a tendency for slip at the wall, evidenced by the following symptoms:

- The density profiles of these liquids can show multiple layers at the metal walls, in accordance with previous experimental findings, which may be attributed to a molecular ordering/packing.
- At the shear rates investigated, the velocity profiles obtained for these systems are almost linear, but with small discontinuity near the walls.
- The corresponding temperature profiles are almost parabolic, but with a small drop at the walls, consistent with the velocity slip.

Compared to equilibrium, alkane chains under shear present higher mean-square end-to-end dimensions at all distances from the wall. In particular, the component of $\langle r^2 \rangle$ in the flow direction is higher than the other two dimensions. This difference in the chain components could be a results of a flattening and/or chain orientation near the walls.

Acknowledgements We wish to thank the Italian MURST and the University of Trieste (Special Grant for Scientific Research) for their financial support.

Appendix

The total potential energy E_p of the COMPASS force field is expressed as a combination of valence terms, including diagonal and off-diagonal cross coupling terms, and nonbonded interaction terms. The analytical form of E_p can then be written as

$$
\begin{aligned}
E_p = & \sum_b \left[K_2(b-b_0)^2 + K_3(b-b_0)^3 + K_4(b-b_0)^4\right] + \sum_\theta \left[H_2(\theta-\theta_0)^2 + H_3(\theta-\theta_0)^3 + H_4(\theta-\theta_0)^4\right] \\
& + \sum_\phi \left\{V_1\left[1-\cos\left(\phi-\phi_1^0\right)\right] + V_2\left[1-\cos\left(2\phi-\phi_2^0\right)\right] + V_3\left[1-\cos\left(3\phi-\phi_3^0\right)\right]\right\} \\
& + \sum_\chi K_\chi \chi^2 \sum_b \sum_{b'} F_{bb'}(b-b_0)\left(b'-b_0'\right) + \sum_\theta \sum_{\theta'} F_{\theta\theta'}(\theta-\theta_0)\left(\theta'-\theta_0'\right) + \sum_b \sum_\theta F_{b\theta}(b-b_0)(\theta-\theta_0) \\
& + \sum_b \sum_\phi (b-b_0)(V_1\cos\phi + V_2\cos 2\phi + V_3\cos 3\phi) + \sum_{b'} \sum_\phi \left(b'-b_0'\right)(V_1\cos\phi + V_2\cos 2\phi + V_3\cos 3\phi) \\
& \times \sum_\theta \sum_\phi (\theta-\theta_0)(V_1\cos\phi + V_2\cos 2\phi + V_3\cos 3\phi) + \sum_\phi \sum_\theta \sum_{\theta'} K_{\phi\theta\theta'}\cos\phi(\theta-\theta_0)\left(\theta'-\theta_0'\right) \\
& + \sum_{i>j} \frac{q_i q_j}{r_{ij}} + \sum_{i>j} E_{ij}\left[2\left(\frac{r_{ij}^0}{r_{ij}}\right)^9 - 3\left(\frac{r_{ij}^0}{r_{ij}}\right)^6\right]
\end{aligned}
$$

References

Andersen HC (1980) Molecular dynamics at constant pressure and/or temperature. J Chem Phys 72:2384–2393

Berendsen HJC, Postma JPM, Van Gunsteren WF, DiNola A, Haak JR (1984) Molecular dynamics with coupling to an external bath. J Chem Phys 81: 3684–3690

Bitsanis I, Magda JJ, Tirrell M, Davis HT (1987) Molecular dynamics of flow in micropores. J Chem Phys 87:1733–1750

Bitsanis I, Somers SA, Davis HT, Tirrell M (1990) Microscopic dynamics of flow in narrow pores. J Chem Phys, 93:3427–3431

Brooks CL III, Montgomery R, Pettitt TB, Karplus M (1985) Structural and energetic effects of truncating long ranged interactions in ionic and polar fluids. J Chem Phys 83:5897–5907

Evans DJ, Morriss GP (1990) Statistical mechanics of non-equilibrium liquids. Academic Press, London, UK

Gao JP, Luedtke WD, Landman U (1997) Origins of solvation forces in confined fluids. J Phys Chem B, 101:4013–4023

Granick S (1999) Soft matter in a tight spot. Phys Today 52:26–31

Kalika DS, Denn MM (1987) Wall slip and extrudate distortion in linear low-

density polyethylene. J Rheol 31:815–834
Khare R, de Pablo J, Yethiraj A (1996) Rheology of confined polymer melts. Macromolecules 29:7910–7918
Luedtke WD, Landman U (1992) Computational material science, vol 1
Rappé AK, Goddard WA III (1991) Charge equilibration for molecular dynamics simulations. J Phys Chem 95:3358–3363
Sun H, Rigby D (1997) Polysiloxanes: ab initio force field and structural, conformational and thermophysical properties. Spectrochim Acta Part A 53: 1301–1310
Verlet L (1967) Computer experiments on classical fluids. I. Thermodynamical properties of Lennard-Jones molecules. Phys Rev 159:98–103
Waldman M, Hagler AT (1993) New combining rules for rare gas van der Waals parameters. J Comput Chem 14:1077–1082